6. Boundary Layers

J. S. Wright
jswright@tsinghua.edu.cn

6.1 Overview

In the previous chapters, we have generally treated the atmosphere and ocean as separate entities. This chapter introduces the concept of boundary layers, and begins to examine the interactions between the atmosphere and ocean in greater detail. Particular attention is paid to the processes that control the fluxes of heat, momentum, and other quantities across the atmosphere–ocean interface. Turbulent mixing and entrainment are introduced and described. The equations of fluid dynamics derived in Chapter 5 are extended to account for the effects of turbulence (along with some useful approximations), and are then used to introduce the concept of Ekman transport. The chapter concludes with independent descriptions of the atmospheric boundary layer and ocean mixed layer.

6.2 What are boundary layers?

The ocean–atmosphere interface encompasses more than just the ocean surface. Boundary layers on both sides of the ocean surface contribute substantially to the exchange of heat, momentum, water, and salt across the ocean surface. Changes in boundary layer conditions directly affect sea surface temperature, which is a crucial component of atmosphere–ocean interactions at scales ranging from very small (molecular diffusion) to very large (the global impacts of El Niño). The surface exchange of aerosols (such as sea salt) and chemical constituents (such as ocean uptake of carbon dioxide or emission of halogen compounds that can accelerate destruction of stratospheric ozone) also depend strongly on boundary layer mixing.

The atmospheric boundary layer is the lowest part of the troposphere. Winds, temperature, and humidity in the atmospheric boundary layer are strongly influenced by conditions at the surface. The depth of the atmospheric boundary layer can vary from a few tens of meters to several kilometers, though it is typically on the order of ~1 km. This depth is determined

primarily by sensible and latent heat fluxes at the surface, which increase or decrease buoyancy in surface air. Sensible heating warms the surface air, while latent heating adds water vapor (which is light relative to dry air). Both processes act to reduce the density of air close to the surface, leading to vertical instability and mixing. Buoyancy-driven mixing in the atmospheric boundary layer is generally strongest in the vertical direction, so that the vertical velocities in these turbulent eddies are typically much larger than the horizontal velocities. The effects of friction reduce the wind speed to near zero at the ocean surface.

The ocean mixed layer is the uppermost part of the ocean. It is in some ways similar to the atmospheric boundary layer: the currents, temperature, and salinity in the ocean mixed layer are profoundly affected by conditions at the ocean surface. However, in contrast to the atmospheric boundary layer, temperature generally decreases with depth (increases with height) in the ocean mixed layer. From a buoyancy perspective, the ocean mixed layer is therefore generally stable (with the important exception of the high latitude ocean during wintertime). The ocean mixed layer is stirred mainly by the mechanical forcing of wind stresses at the surface. The same frictional effects that reduce wind speeds to near zero in the surface atmosphere transfer momentum into the ocean mixed layer. The mechanical forcing of this momentum flux forms eddies that stir the surface ocean. The depth of the ocean mixed layer (typically ~20–50 m) is therefore primarily determined by the magnitude of the wind stress at the ocean surface. Unlike turbulent eddies in the atmospheric boundary layer, the vertical and horizontal velocities in wind-driven eddies in the ocean mixed layer are generally of similar magnitude.

Boundary layers on both sides of the ocean surface respond rapidly to changes in surface conditions. For this reason, the diurnal cycle is generally strong in the atmospheric boundary layer relative to the free atmosphere, while the seasonal cycle is strong in the ocean mixed layer relative to the deep ocean.

The atmospheric and oceanic boundary layers are well-mixed when turbulent mixing is strong. Under these conditions, quantities such as potential temperature, water vapor, and salinity are approximately independent of height or depth within the boundary layer. The ocean–atmosphere boundary is illustrated schematically in Fig. 6.1. Potential temperature is generally well-mixed within the atmospheric boundary layer and ocean mixed layer. Above the atmospheric boundary layer, potential temperature increases according to the lapse rate in the free atmosphere (Section 2.2.2). Below the ocean mixed layer, temperature gradually decreases in the thermocline (Section 2.3.1). The momentum flux is directed downward from the free atmosphere (where winds are relatively strong) through the atmospheric boundary layer (where winds decrease due to the effects of friction at the surface) and into the ocean (where the surface winds drive eddies and ocean currents). The flux of water vapor is upward from the evaporative source at the ocean surface. Turbulent eddies in the atmospheric boundary layer rapidly mix warm, moist air up from the surface and replace it with relatively cool, dry air from higher levels. This process dramatically increases the fluxes of heat and moisture into the atmosphere.

6.3 THE SURFACE ENERGY BUDGET

The net heat flux into the ocean surface Q_{NET} can be written as

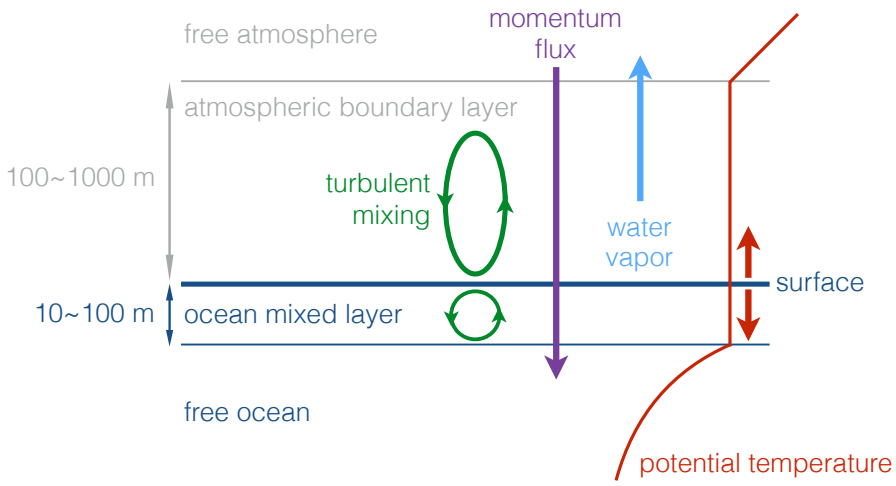

Figure 6.1: Schematic diagram of the atmosphere–ocean interface. Interactions between the atmosphere and ocean occur mainly between the ocean mixed layer and the atmospheric boundary layer. Fluxes of momentum, heat, and water vapor between the atmosphere and ocean pass through these boundary layers, and are accelerated substantially by turbulent mixing.

$$Q_{\mathrm{NET}} = Q_{\mathrm{SW}} - Q_{\mathrm{LW}} - Q_{\mathrm{LH}} - Q_{\mathrm{SH}}, \tag{6.1}$$

where Q_{SW} is the flux of solar radiation into the surface (positive downward), Q_{LW} is the net flux of long-wave radiation out of the surface (positive upward), Q_{LH} is the evaporative latent heat flux into the atmosphere (positive upward), and Q_{SH} is the sensible heat flux into the atmosphere (positive upward). The first two terms on the right hand side of Eq. 6.1 are often combined into the net radiative flux $Q_{\mathrm{RAD}} = Q_{\mathrm{SW}} - Q_{\mathrm{LW}}$. All fluxes are typically expressed in units of $\mathrm{W\,m^{-2}}$. These energy fluxes were introduced and briefly discussed in Section 1.3, and their global mean magnitudes are shown in Fig. 1.13. Here, we focus on the sensible and latent heat fluxes, which are strongly affected by turbulent mixing in the boundary layer.

6.3.1 Sensible and latent heating

Sensible heating is produced by the direct heating (or cooling) of air in contact with the surface. If the surface is warmer than the air immediately above it, the sensible heat flux will act to warm the air and cool the surface. Conversely, if the surface is cooler than the air immediately above it, the sensible heat flux will act to cool the air and warm the surface. Above the surface, sensible heating is accomplished by turbulent mixing. A vertical sensible heat flux results when the air moving upward in a turbulent eddy has a different potential temperature than the air moving downward. The time mean sensible heat flux can be expressed as

$$Q_{\mathrm{SH}} = c_p \rho_a \overline{w\theta}, \tag{6.2}$$

where c_p is the specific heat of air at constant pressure, ρ_a is the density of the air, and $\overline{w\theta}$ is the time average product of vertical velocity and potential temperature.

In climate physics, the latent heat flux refers to the energy exchanged between the surface and the atmosphere in the form of evaporation. Like the sensible heat flux, the latent heat flux may be negative if water vapor condenses directly from the atmosphere onto the surface (in the form of dew or frost). The "latent" in latent heat flux refers to the fact that this energy flux does not involve an explicit transfer of heat between the surface and atmosphere. Evaporation removes energy from the surface, but that energy is only delivered to the atmosphere when the evaporated water vapor condenses into liquid water or ice. The physical process of evaporation occurs at the molecular level within the lowest millimeter of the atmosphere. Above this layer, a latent heat flux results when the air moving upward in a turbulent eddy has a different water vapor concentration than the air moving downward. The time mean latent heat flux can by expressed as

$$Q_{\mathrm{LH}} = L_v \rho_a \overline{wq} \tag{6.3}$$

where L_v is the latent heat of vaporization and q is the specific humidity.

6.3.2 The Bowen ratio

The latent heat flux over the ocean depends on sea surface temperature and the relative humidity of surface air, and is strongly influenced by the ocean currents and upwelling of cold water to the surface (which reduces sea surface temperatures and limits the latent heat flux). The Bowen ratio B is defined as the ratio of sensible heating to latent heating

$$B \equiv \frac{Q_{\mathrm{SH}}}{Q_{\mathrm{LH}}}. \tag{6.4}$$

Over the oceans, where the water available for evaporation is practically unlimited, the Bowen ratio is generally small. The maximum theoretical Bowen ratio for a given temperature, also called the equilibrium Bowen ratio (B_e), results when the air immediately above the surface is saturated (i.e., the relative humidity equals one):

$$B_e^{-1} = \frac{L_v}{c_p} \frac{\partial q^*}{\partial T}, \tag{6.5}$$

where $q*$ is the saturation mixing ratio and we have assumed that changes in potential temperature near the surface are dominated by changes in surface air temperature rather than changes in surface pressure. The Bowen ratio above the ocean (or any wet surface) is always equal to or smaller than B_e.

6.3.3 REYNOLDS AVERAGING

Equations 6.2 and 6.3 express the sensible and latent heat fluxes in terms of time mean quantities ($\overline{w\theta}$ and $\overline{wq}$). These expressions are only valid if the data used to calculate these time mean quantities are available at frequent enough intervals to fully characterize the turbulent fluctuations that produce the vertical transport in both time and space. Turbulent fluctuations can be very rapid (faster than 1 s), and it is generally not possible to adequately characterize the turbulent fluxes. The effects of turbulent eddies on the large-scale flow can be represented in a time mean sense, however. This is accomplished by first separating each variable into time mean and fluctuating components (e.g., $w = \overline{w} + w'$ and $\theta = \overline{\theta} + \theta'$). This procedure is called Reynolds averaging, after the fluid dynamicist Osborne Reynolds. Using Reynolds averaging, we have

$$\overline{w\theta} = \overline{(\overline{w} + w')(\overline{\theta} + \theta')} = \overline{w}\,\overline{\theta} + \overline{w'\theta'}, \tag{6.6}$$

The terms in which a fluctuation is multiplied by a time mean component disappear. To confirm this, note that $\overline{w'\overline{\theta}}$ simplifies to $\overline{w'} \cdot \overline{\theta}$, which equals zero because the time average of the fluctuation component w' is zero.

The sensible and latent heat fluxes can then be rewritten in Reynolds form as

$$Q_{\mathrm{SH}} = c_p \rho_a (\overline{w}\,\overline{\theta} + \overline{w'\theta'}) \approx c_p \rho_a \overline{w'\theta'} \tag{6.7}$$

$$Q_{\mathrm{LH}} = L_v \rho_a (\overline{w}\,\overline{q} + \overline{w'q'}) \approx L_v \rho_a \overline{w'q'}. \tag{6.8}$$

The approximations result from assuming that the mean vertical velocity is small relative to the typical vertical velocity in turbulent eddies. The fluctuation terms in these equations are rarely measured, and are not explicitly simulated in climate models. In practice, the turbulent sensible and latent heat fluxes must be estimated using variables averaged over larger spatial scales and longer time scales than the turbulent motions themselves. The bulk aerodynamic formulae are one example. These formulae parameterize the strength of turbulent energy transfer based on conditions at some reference height z_r:

$$Q_{\mathrm{SH}} = c_p \rho_a C_{\mathrm{D,SH}} \overline{V}(z_r) \left[\theta(z_0) - \theta(z_r)\right] \tag{6.9}$$

$$Q_{\mathrm{LH}} = L_v \rho_a C_{\mathrm{D,LH}} \overline{V}(z_r) \left[q(z_0) - q(z_r)\right] \tag{6.10}$$

where $\overline{V}(z_r)$ is the mean wind speed at the reference height, $\left[\theta(z_0) - \theta(z_r)\right]$ and $\left[q(z_0) - q(z_r)\right]$ are the vertical differences of potential temperature and humidity between the surface and the reference height, and $C_{\mathrm{D,SH}}$ and $C_{\mathrm{D,LH}}$ are the dimensionless drag (or aerodynamic transfer) coefficients for temperature and humidity, respectively. The drag coefficients for temperature and humidity are typically approximately equal. Their magnitudes depend on surface roughness, stability, and the reference height.

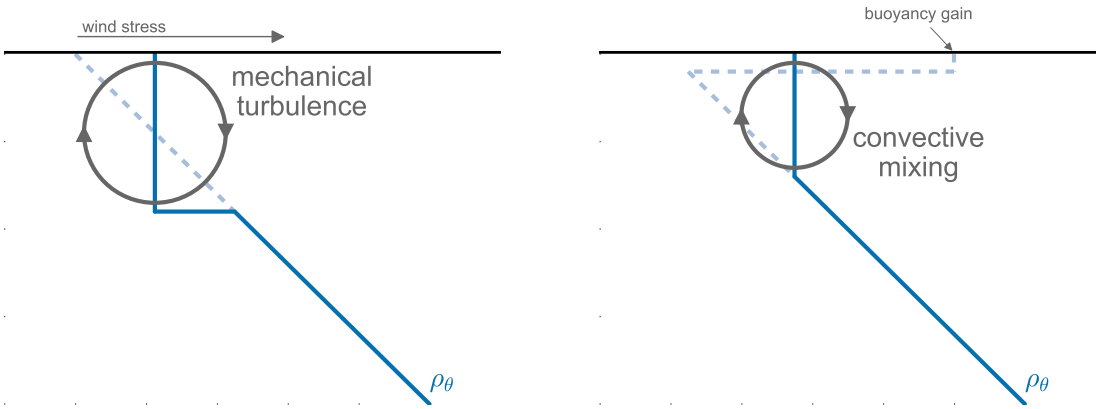

Figure 6.2: Schematic illustrations of mixing in a stably stratified ocean surface layer due to (left) mechanical forcing and (right) buoyancy instability.

6.4 Turbulent mixing, inversions, and entrainment

Turbulent mixing in boundary layers has two main forms. Mechanical turbulence is generated by the conversion of horizontal momentum to turbulent motion, and is strongest when the vertical gradient of horizontal wind (the vertical wind shear) is strong. Convective turbulence is generated when the vertical profile of buoyancy is unstable, as discussed in Section 2.4.2. Turbulence is both irregular and chaotic, with random motion at a wide range of spatial and temporal scales.

6.4.1 Entrainment

Suppose we introduce a wind stress at the ocean surface. This wind stress creates a mechanical instability that mixes an otherwise stable profile of potential density in the ocean between the surface and a depth d_m. The resulting potential density profile contains a discontinuity at the depth d_m, as shown in Fig. 6.2. Discontinuities of this type are characteristic of the interfaces between relatively well-mixed turbulent layers and neighboring stably stratified layers (such as the interface between the atmospheric boundary layer and the free troposphere, the interface between the troposphere and the stratosphere, or the boundary between the ocean mixed layer and the thermocline). If the wind stress increases, it will strengthen the turbulent eddies in the ocean mixed layer. If the turbulence has enough energy to overcome the discontinuity, it will invade the denser stably stratified fluid. The turbulent elements will entrain (draw in) some of the stably stratified fluid, increasing the depth of the mixed layer. This process is called entrainment.

The entrainment velocity w_e is defined as the rate per unit area at which the denser stably stratified fluid is drawn into the turbulent boundary layer (i.e., the flux of fluid out of the stable layer and into the turbulent layer). For the ocean (where the stably stratified layer is located below the turbulent layer), the entrainment velocity must be directed upward for the

ocean mixed layer to grow. By contrast, for the atmosphere (where the stably stratified layer is located above the turbulent layer), the entrainment velocity must be directed downward for the atmospheric boundary layer to grow. The change in the depth of the mixed layer bottom is given by

$$\frac{d(d_m)}{dt} = w - w_e, \tag{6.11}$$

where $w = \frac{dz}{dt}$ is the large-scale vertical velocity as defined in Chapter 3. If there is no entrainment, $w_e = 0$ and the mixed layer bottom moves according to the mean upwelling or downwelling in the surrounding ocean. In this case, changes in the depth of the local mixed layer are balanced by horizontal convergence or divergence. If $w_e > w$, then entrainment will increase the depth of the turbulent mixed layer. Conversely, if $w_e < w$ then entrainment will decrease the depth of the turbulent mixed layer (this process may also be called detrainment). The depth of the mixed layer remains constant in the special case where $w_e = w$, in which case the addition (or loss) of fluid by entrainment exactly balances the loss (or addition) of fluid by divergence (convergence).

6.4.2 Turbulent kinetic energy

Changes in the properties of the boundary layer result from a combination of four factors: the depth or height of the boundary layer, the magnitude of the discontinuity at the interface, the entrainment rate w_e, and the source of energy for the turbulence. The first two factors can be derived from Eq. 6.11 and the assumption of a well-mixed boundary layer, respectively. The turbulent kinetic energy (TKE) can be defined as

$$\text{TKE} \equiv \frac{\overline{u'^2} + \overline{v'^2} + \overline{w'^2}}{2}. \tag{6.12}$$

Its time rate of change can be expressed as

$$\frac{d(\text{TKE})}{dt} = \text{MP} + \text{BPL} + \text{TR} - \varepsilon, \tag{6.13}$$

where MP represents mechanical production (by, e.g., wind shear instabilities or wind stresses at the ocean surface), BPL represents buoyancy production and loss (e.g., exchange of sensible and latent heat), TR represents transport (e.g., transfer of kinetic energy from eddies with larger spatial scales or longer time scales), and ε represents frictional dissipation. This expression indicates that the ultimate source of energy for turbulent mixing (and associated entrainment) is typically either a mechanical forcing (as in the case of the tropical ocean mixed layer), a buoyancy flux (as in the case of the tropical atmospheric boundary layer), or a cascade of energy from large-scale eddies (such as large weather systems). The primary sink of TKE is frictional dissipation. The frictional dissipation of turbulent kinetic energy is strong. As a result, turbulent motion will quickly decay without a constant supply of energy.

At the atmosphere–ocean interface, the atmospheric boundary layer tends to be deeper when the surface is being heated and the winds are strong, while the ocean mixed layer tends to be deeper when the surface is being cooled and the winds are strong. Both situations correspond to positive BPL (buoyancy production) and positive MP (mechanical production).

6.5 FLUID DYNAMICS FOR BOUNDARY LAYERS

6.5.1 TURBULENT DISSIPATION

Turbulence requires some modifications to the momentum equations. It helps to start by rewriting the momentum equations using the Boussinesq approximation (i.e., $\rho = \rho_0$ everywhere except where coupled with gravity, with ρ_0 a constant; Section 5.4.4). For example, the left hand side of the zonal momentum equation can be rewritten as

$$\begin{aligned}\frac{\partial u}{\partial t} + (\mathbf{v}\cdot\nabla)u &= \frac{\partial u}{\partial t} + (\mathbf{v}\cdot\nabla)u + u\left(\frac{\partial u}{\partial x} + \frac{\partial v}{\partial y} + \frac{\partial w}{\partial z}\right) \\ &= \frac{\partial u}{\partial t} + u\frac{\partial u}{\partial x} + v\frac{\partial u}{\partial y} + w\frac{\partial u}{\partial z} + u\left(\frac{\partial u}{\partial x} + \frac{\partial v}{\partial y} + \frac{\partial w}{\partial z}\right) \\ &= \frac{\partial u}{\partial t} + \frac{\partial u^2}{\partial x} + \frac{\partial uv}{\partial y} + \frac{\partial uw}{\partial z}\end{aligned}$$

where we have used the fact that the Boussinesq system is non-divergent (Eq. 5.46), such that

$$\frac{\partial u}{\partial x} + \frac{\partial v}{\partial y} + \frac{\partial w}{\partial z} = 0.$$

Using Reynolds averaging, we can then express the turbulent zonal momentum equation as

$$\begin{aligned}\overline{\frac{\partial u}{\partial t} + (\mathbf{v}\cdot\nabla)u} &= \frac{\partial \overline{u}}{\partial t} + \frac{\partial}{\partial x}(\overline{u}\,\overline{u} + \overline{u'u'}) + \frac{\partial}{\partial y}(\overline{u}\,\overline{v} + \overline{u'v'}) + \frac{\partial}{\partial z}(\overline{u}\,\overline{w} + \overline{u'w'}) \\ &= \frac{\partial \overline{u}}{\partial t} + (\overline{\mathbf{v}}\cdot\nabla)\overline{u} + \frac{\partial}{\partial x}(\overline{u'u'}) + \frac{\partial}{\partial y}(\overline{u'v'}) + \frac{\partial}{\partial z}(\overline{u'w'})\end{aligned}$$

Applying the same procedure to all of the momentum equations yields

$$\frac{\partial \overline{u}}{\partial t} + (\overline{\mathbf{v}}\cdot\nabla)\overline{u} + \frac{\partial}{\partial x}(\overline{u'u'}) + \frac{\partial}{\partial y}(\overline{u'v'}) + \frac{\partial}{\partial z}(\overline{u'w'}) = -\frac{1}{\rho_0}\frac{\partial \overline{p}}{\partial x} + f\overline{v} + \overline{F_x} \tag{6.14}$$

$$\frac{\partial \overline{v}}{\partial t} + (\overline{\mathbf{v}}\cdot\nabla)\overline{v} + \frac{\partial}{\partial x}(\overline{v'u'}) + \frac{\partial}{\partial y}(\overline{v'v'}) + \frac{\partial}{\partial z}(\overline{v'w'}) = -\frac{1}{\rho_0}\frac{\partial \overline{p}}{\partial y} - f\overline{u} + \overline{F_y} \tag{6.15}$$

$$\frac{\partial \overline{w}}{\partial t} + (\overline{\mathbf{v}}\cdot\nabla)\overline{w} + \frac{\partial}{\partial x}(\overline{w'u'}) + \frac{\partial}{\partial y}(\overline{w'v'}) + \frac{\partial}{\partial z}(\overline{w'w'}) = -\frac{1}{\rho_0}\frac{\partial \overline{p}}{\partial z} + b + \overline{F_z}. \tag{6.16}$$

Using a similar approach, the thermodynamic equation (expressed in terms of the buoyancy b) becomes

$$\frac{\partial \overline{b}}{\partial t} + (\overline{\mathbf{v}}\cdot\nabla)\overline{b} + \frac{\partial}{\partial x}(\overline{u'b'}) + \frac{\partial}{\partial y}(\overline{u'b'}) + \frac{\partial}{\partial z}(\overline{u'b'}) = \dot{b} \tag{6.17}$$

where $\dot{b}$ collects changes in buoyancy due to diabatic heating (changes in θ) and changes in composition (e.g., salinity or humidity).

Over the ocean, there is little horizontal variability in surface roughness. As a consequence, we can generally neglect all terms involving $\partial/\partial x$ or $\partial/\partial y$. In this case, the fluid dynamical equations for turbulent boundary layers only include turbulent fluxes that involve $\partial/\partial z$. For example, the horizontal momentum equations can be written as

$$\frac{\partial \overline{u}}{\partial t} + (\overline{\mathbf{v}} \cdot \nabla)\overline{u} = -\frac{1}{\rho_0}\frac{\partial \overline{p}}{\partial x} + f\overline{v} - \frac{\partial \overline{u'w'}}{\partial z} \tag{6.18}$$

$$\frac{\partial \overline{v}}{\partial t} + (\overline{\mathbf{v}} \cdot \nabla)\overline{v} = -\frac{1}{\rho_0}\frac{\partial \overline{p}}{\partial y} - f\overline{u} - \frac{\partial \overline{v'w'}}{\partial z} \tag{6.19}$$

$$\tag{6.20}$$

where the turbulent terms take the place of the frictional term. In Chapter 5, we learned that the frictional term in the momentum equations is often used to account for momentum generation or dissipation that occurs at space or time scales that are too small to resolve. Turbulent momentum transfer in boundary layers is one such process. Note also that taking the terms on the left-hand side to be zero corresponds to quasi-geostrophic balance, the three-way balance between the pressure gradient force, the Coriolis force, and turbulent (frictional) dissipation.

The new fluid dynamical equations now include several new unknowns (under the Boussinesq approximation, at least four: u', v', w', and θ'). One approximation that allows us to again generate a closed set of equations (i.e., seven equations for seven unknowns) is the flux-gradient approximation (also known as K theory). Under the flux-gradient approximation, turbulent eddies are assumed to act like molecular diffusion, so that the turbulent flux of a given quantity is proportional to the local gradient of the mean field:

$$\overline{u'w'} = -K_M\left(\frac{\partial \overline{u}}{\partial z}\right), \quad \overline{v'w'} = -K_M\left(\frac{\partial \overline{v}}{\partial z}\right), \quad \overline{\theta'w'} = -K_H\left(\frac{\partial \overline{\theta}}{\partial z}\right)$$

where K_M is the eddy diffusivity of momentum and K_H is the eddy diffusivity of heat (also often used to represent the eddy diffusivity of water vapor). This closure scheme has a number of limitations. In particular, the eddy diffusivities depend on the state of the flow rather than the physical properties of the fluid, and must be determined empirically for each situation.

6.5.2 Wind stress

The momentum flux between the atmosphere and ocean is determined primarily by the wind stress. The wind stress at the surface of the ocean is described by the equations

$$\tau_x = -\rho_a\overline{(w'u')} \tag{6.21}$$

$$\tau_y = -\rho_a\overline{(w'v')} \tag{6.22}$$

so that the two-dimensional wind stress vector is given by the vector equation

$$\tau_{xy} = -\rho_a \overline{(w'\mathbf{u}')} \tag{6.23}$$

For a given stress at the ocean surface, the friction velocity $u_\star$ is defined as the ratio of the vector magnitude of the surface stress to the density of the fluid

$$u_\star^2 \equiv \frac{|\tau_{xy}|}{\rho}, \tag{6.24}$$

In this formulation, $u_\star$ describes the velocity characteristic of the stress in a fluid of density ρ. The surface stress is continuous from the atmosphere to the ocean, so that

$$|\tau_{xy}| = (\rho u_\star^2)_{\text{air}} = (\rho u_\star^2)_{\text{ocean}} \tag{6.25}$$

The mean vertical profile of horizontal wind can generally be expressed as

$$\overline{u(z)} = \frac{u_\star}{\kappa} \ln\left(\frac{z}{z_0}\right), \tag{6.26}$$

where $u_\star$ is the friction velocity, $\kappa = 0.4$ is the von Karman constant, and z_0 is the roughness coefficient. Thus the vertical gradient of the horizontal wind speed can typically be used to determine both the friction velocity $u_\star$ and the surface wind stress τ. Over the ocean, the roughness coefficient z_0 can also be determined based on the friction velocity $u_\star$:

$$z_0 = \frac{\alpha u_\star^2}{g}, \tag{6.27}$$

where g is the acceleration due to gravity and $\alpha = 0.016$ is the Charnock constant. This quantity represents the roughness of the ocean (i.e., the height of the waves).

The introduction to boundary layer dynamics given here is far from exhaustive. For more information about the dynamics of boundary layers, see in particular *Holton* (1992) or *Vallis* (2006). Most global-scale models parameterize boundary layer dynamics to a substantial extent. For an introduction to some parameterization techniques for the atmospheric boundary layer and ocean mixed layer, see *Jacobson* (2005) or *Sarachik and Cane* (2010).

6.6 Ekman flow

Although the flux-gradient approximation is not suitable for most purposes in computational fluid dynamics, it can still be used to derive powerful insight into the boundary layer dynamics. For instance, assuming geostrophic balance at the top of the boundary layer, the flux-gradient forms of Eqs. 6.18 and 6.19 can be used to derive the equations for the classical Ekman layer:

$$K_M \frac{\partial^2 \overline{u}}{\partial z^2} + f(\overline{v} - \overline{v_g}) = 0 \tag{6.28}$$

$$K_M \frac{\partial^2 \overline{v}}{\partial z^2} - f(\overline{u} - \overline{u_g}) = 0 \tag{6.29}$$

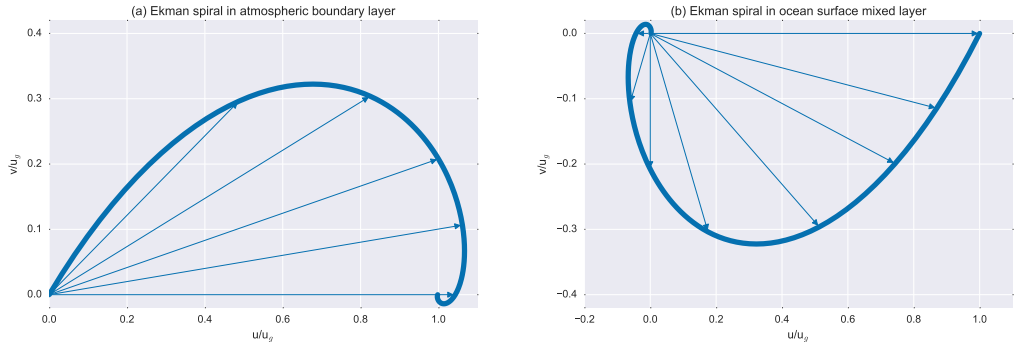

Figure 6.3: Ekman spirals in the Northern Hemisphere (a) atmospheric boundary layer (relative to a purely zonal geostrophic flow at the base of the free atmosphere) and (b) ocean surface mixed layer (relative to a purely zonal surface flow).

Assuming $v_g = 0$ (i.e., orienting the flow in the zonal direction), these equations can be solved to yield the height dependence of the wind field in the Northern Hemisphere atmospheric boundary layer relative to the geostrophic winds at the base of the free atmosphere (for a more detailed derivation, see *Vallis*, 2006):

$$\overline{u} = \overline{u_g}\left[1 - e^{-\gamma z}\cos(\gamma z)\right]$$
$$\overline{v} = \overline{u_g}\left[e^{-\gamma z}\sin(\gamma z)\right]$$

As height decreases from the boundary layer top, the horizontal winds grow weaker and are redirected progressively to the left of the geostrophic wind (Fig. 6.3a). The counter-clockwise rotation of the horizontal winds results from the three-way balance between the pressure gradient force (which is directed across the geostrophic wind vector, oriented left-to-right in this plot), the Coriolis force (which is directed to the right of the flow with a magnitude proportional to the wind speed), and the frictional component (which grows larger closer to the surface). The wind vectors close to the surface are oriented increasingly along the pressure gradient as the Coriolis force decreases.

The equivalent vertical variation of currents in the Northern Hemisphere ocean mixed layer (Fig. 6.3b) can be derived as

$$\overline{u} = \overline{u_g}\left[e^{-\gamma z}\cos(\gamma z)\right]$$
$$\overline{v} = \overline{u_g}\left[-e^{-\gamma z}\sin(\gamma z)\right]$$

The surface wind exerts a force on the surface of the ocean that is oriented left-to-right. If the pressure gradient is negligible, then the surface wind stress must be balanced by the frictional

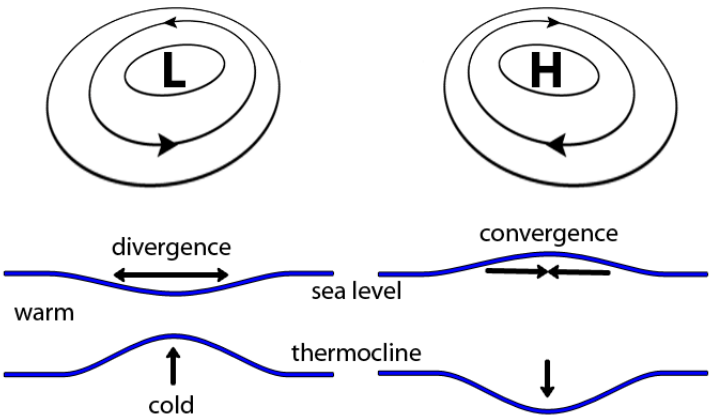

Figure 6.4: Schematic diagram of Ekman suction (left) and Ekman pumping (right) in the ocean mixed layer under atmospheric circulation systems. The situation in the ocean mixed layer mirrors that in the atmosphere, where ageostrophic cyclonic flow around a low is associated with Ekman pumping (rising motion) and ageostrophic anticyclonic flow around a high is associated with Ekman suction (subsidence).

stress at the base of the surface layer (which acts in the opposite direction) and the Coriolis force (which acts to the right of the flow). This three-way balance of forces results in a surface flow that is oriented to the right of the initial surface stress. This surface flow exerts a slightly weaker stress on the layer immediately below the surface layer, resulting in a second three-way balance of forces that produce a flow in the second layer that is oriented slightly to the right of the flow in the surface layer. This flow in turn exerts a stress on the next layer down, which drives another flow that exerts a stress on the layer below that, and so on. The Ekman spiral in the Northern Hemisphere surface ocean rotates clockwise from the surface flow.

The integrated Ekman mass transport is oriented perpendicular to the surface wind stress. In the Northern Hemisphere, the quasi-geostrophic flow associated with a cyclonic (low-pressure) weather system is oriented approximately counter-clockwise. The surface stress associated with this counter-clockwise flow will lead to divergence in the ocean surface layer (Fig. 6.4). Conservation of mass dictates that this divergence be balanced by upwelling of colder water from deeper layers. Tropical cyclones can dramatically reduce sea surface temperatures by inducing strong upwelling. The opposite situation occurs under anticyclonic (high-pressure) systems, which impart a clockwise wind stress. This clockwise wind stress forces convergence, which must be balanced by downwelling.

Ekman spirals are rarely observed in the atmosphere and ocean (due to strong time variability in wind stress, other forces that are not included in the theory, and the difficulty of observing vertical profiles of winds and/or currents). Moreover, Ekman flow is weak outside of relatively shallow boundary layers in the ocean and atmosphere. The most important effect of Ekman flow is that it creates convergence or divergence in the boundary layer, which by conservation of mass drives Ekman pumping or suction. These impacts on the vertical flow

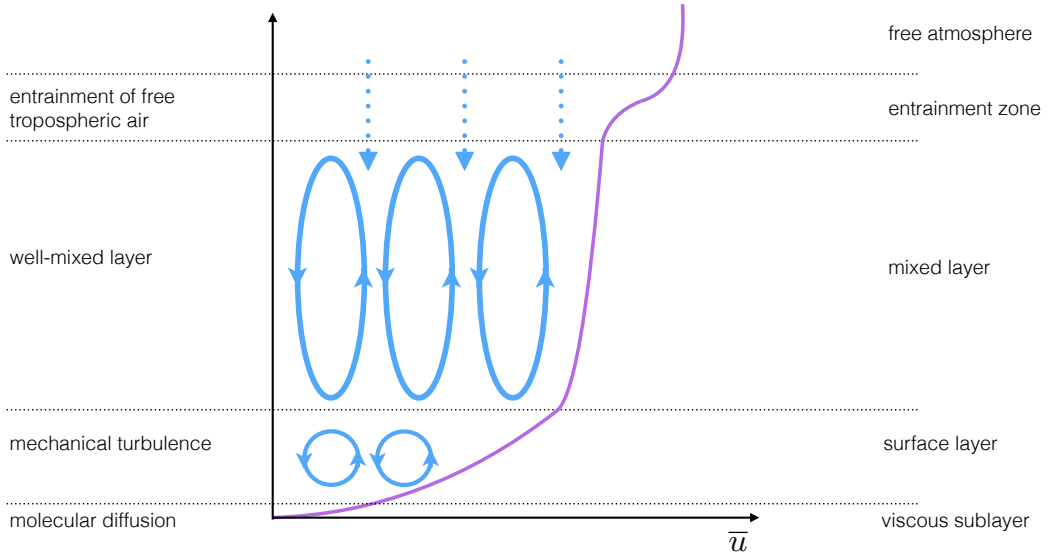

Figure 6.5: Schematic diagram of the structure of a convective atmospheric boundary layer, with a viscous sublayer dominated by molecular diffusion, a surface mixed dominated by mechanical turbulence, a well-mixed boundary layer with a combination of forced and free convection, and an entrainment zone transitioning to the free toposphere above. The flow in the free atmosphere is generally assumed to be geostrophic.

drive much of the vertical motion in the fluid, and contribute substantially to the development of secondary flows outside of the Ekman layer itself.

6.7 The atmospheric boundary layer

The structure of the atmospheric boundary layer varies substantially depending on a number of factors, including the surface roughness, ambient vertical and horizontal winds, temperature and moisture advection, and time of day (i.e., whether Q_{RAD} is heating or cooling the surface). The atmospheric boundary layer tends to deepen during the daytime, when solar radiation heats the surface, increases Q_{SH} and Q_{LH}, and produces TKE (via the BPL term in Eq. 6.13). The atmospheric boundary layer tends to be shallower at night, when the surface cools by long-wave radiation. The nighttime boundary layer is generally maintained by mechanical production of TKE due to the increase in the horizontal wind speed with height (the vertical shear of horizontal wind).

The lowest layer of the atmospheric boundary layer is the surface layer, where frictional effects are largest (Fig. 6.5). The surface layer accounts for no more than about 10% of the total depth of the atmospheric boundary layer. Turbulence in the surface layer is largely mechanical in origin, and is caused by strong vertical shear in the horizontal wind. The vertical fluxes of momentum, heat, and moisture are nearly constant in the surface layer. Above the surface

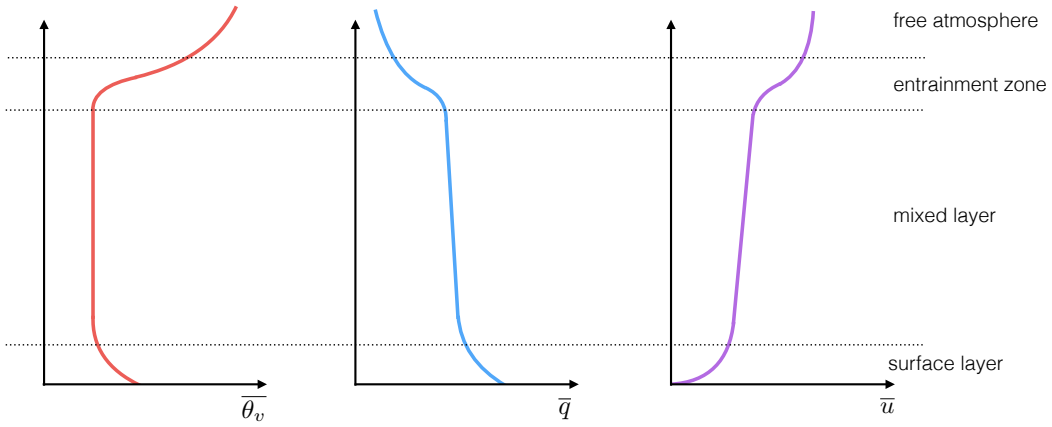

Figure 6.6: Schematic diagram of the vertical variations of mean virtual potential temperature, specific humidity and horizontal wind in a convective atmospheric boundary layer.

layer is the atmospheric mixed layer, where turbulence may be either mechanically-driven or buoyancy-driven. This layer is by definition well-mixed, and the vertical profiles of potential temperature, specific humidity, and momentum are therefore approximately constant with height. In mid-latitudes, the Coriolis force becomes important in the mixed layer. The effects of both turbulence and rotation must be accounted for in this case, and lead to the development of an Ekman layer above the surface layer. A transitional entrainment zone connects the turbulent boundary layer to the free atmosphere above. Motion in the free atmosphere is largely decoupled from friction, and is therefore approximately geostrophic in most cases.

Through most of the atmospheric boundary layer, turbulence can be either mechanical or thermal in origin (Fig. 6.5). Convective mixing resulting from mechanical forcings (e.g., vertical wind shear or surface roughness) is generally referred to as forced convection, while convective mixing resulting from thermal forcings (e.g., buoyancy fluctuations) is referred to as free convection. The stability of the atmosphere in the presence of vertical wind shear is no longer a function of potential temperature alone, and may be represented by the Richardson number

$$R_\mathrm{i} = \frac{g}{\overline{\theta}} \frac{\partial \overline{\theta}/\partial z}{(\partial \overline{\mathbf{u}}/\partial z)^2}. \tag{6.30}$$

The Richardson number is equal to the static stability N^2 (Eq. 4.3) over the square of the vertical shear of horizontal wind. The Richardson number fundamentally represents the ratio between the destruction of TKE by buoyancy forces and the generation of TKE by wind shear. Smaller values of R_i therefore correspond to stronger turbulence, with negative values indicating strong turbulence (just as negative values of N^2 indicate dry convective instability). Neglecting the effects of frictional dissipation, turbulent motion can be maintained when $R_\mathrm{i} \leq 1$. Taking into account the effects of frictional dissipation, the critical value of R_i is approximately 0.25.

Clouds in the atmospheric boundary layer may affect vertical transport and boundary layer

physics. Latent heat release during cloud formation can strengthen turbulent motion by producing buoyancy (and therefore TKE). The radiative effects of clouds also have important implications for turbulent motion. For example, fog can reduce the amount of solar radiation reaching the surface, which may in turn reduce the production of TKE by placing stronger limits on Q_{SH} and Q_{LH}. By contrast, long-wave radiative cooling at the top of low stratocumulus clouds can generate buoyancy by cooling the air at the top of the boundary layer, which then sinks and is replaced by warmer air rising from below. The bases of most boundary layer clouds (with the exception of fog) are generally well above the surface, so that the presence of clouds may separate the boundary layer into cloud and sub-cloud layers.

6.8 THE OCEAN MIXED LAYER

The solar flux and heating rate decrease approximately exponentially with depth in the ocean. Over 55% of the solar energy that reaches the ocean is absorbed in the top meter, and almost all of the solar energy flux into the ocean is absorbed within the top 100 m. The ocean mixed layer is therefore strongly stabilized by solar heating at the sea surface. On the other hand, while solar absorption occurs throughout the depth of the mixed layer, the corresponding fluxes of energy out of the ocean (sensible heat, latent heat, and long-wave radiation) occur almost exclusively at the sea surface. This means that solar absorption must be balanced by some upward flux of energy. Molecular diffusion is important within the top centimeter of the ocean, but the remainder must be accounted for by mean vertical motion (upwelling and downwelling), convection, and turbulent mixing. Turbulent and convective mixing in the ocean are so efficient that temperature and salinity are almost uniform within the mixed layer.

Figure 6.7 illustrates the processes that are important in the ocean mixed layer. The depth of the mixed layer depends on the rate of buoyancy generation and the rate at which the surface wind stress supplies kinetic energy. Because of the strong stability of the surface ocean, turbulence in the ocean mixed layer is primarily mechanically generated by wind stresses at the ocean surface. One important exception occurs at high latitudes during autumn and winter, when rapid surface cooling generates unstable buoyancy profiles. In this case, convection rapidly mixes cold, dense surface waters into the deeper ocean. This high latitude convection plays an important role in driving the deep ocean ocean circulation. Weaker surface cooling also produces buoyancy and encourages vertical mixing. Buoyancy can also be generated in the surface mixed layer by increases of salinity due to strong evaporation or transport. Rainfall has the opposite effect, freshening and decreasing the density of surface waters (and therefore increasing the static stability).

The ocean mixed layer is thin (only a few meters) in regions that experience strong solar heating, frequent precipitation, or upwelling from below (such as along the equator or in the eastern boundary currents), and is thick (even up to the depth of the ocean) in regions where Q_{NET} is negative or salinity is high (such as at high latitudes, particularly in the Norwegian Sea). The global mean depth of the ocean mixed layer is approximately 70 m. Relative to the rest of the ocean, the mixed layer responds rapidly to changes in surface conditions (as we have seen from the two-box ocean model introduced in Section 3.4.3). On time scales of less than ten years, the heat capacity of the mixed layer represents almost the entire heat capacity of the ocean. Despite the relatively shallow depth of the mixed layer, this heat capacity is many

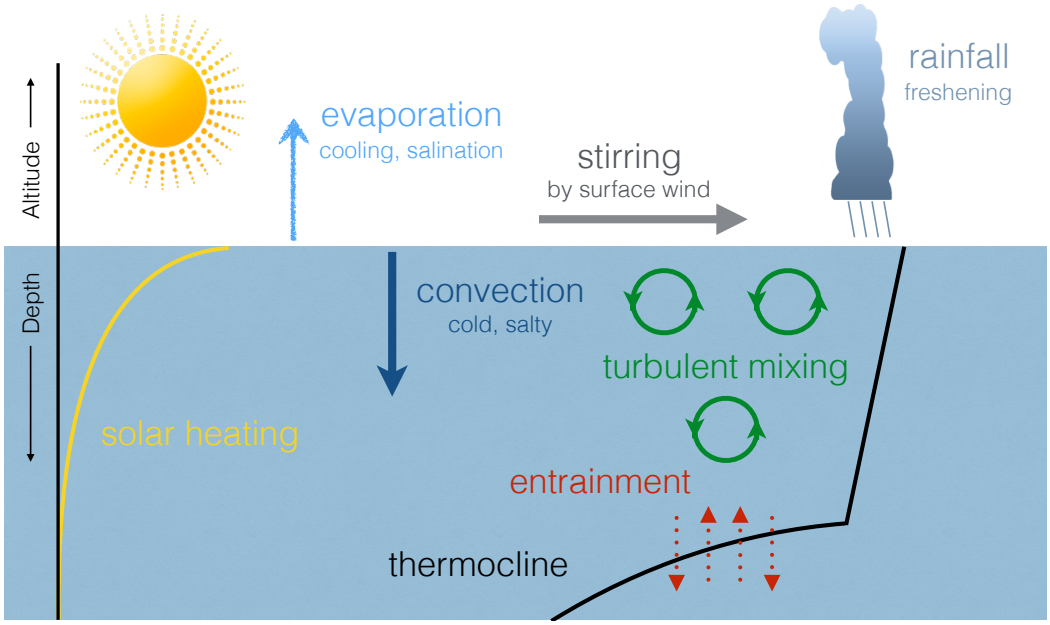

Figure 6.7: Schematic diagram showing important processes in the ocean mixed layer.

times that of the atmosphere.

Figure 6.8 shows the annual cycle of temperature in the upper 110 m of the Pacific Ocean near 40°N. The mixed layer is shallowest (less than 20 m) during late summer, when the destruction of buoyancy by solar heating is strongest and mixing by surface winds is weakest. The mixed layer is deepest (greater than 100 m) during winter and early spring, when solar heating is weak and the surface wind stress is large. These changes reflect the general effects of surface heating and cooling on the depth of the mixed layer. Surface heating reduces the density at the ocean–atmosphere interface. If this modified density profile is then mixed by the wind, the resulting mixed layer will tend to be shallower than the initial one. The opposite occurs with surface cooling, which increases the density of the water near the interface: wind-driven mixing will then tend to result in a deepening of the mixed layer.

The strength of turbulence in the ocean mixed layer can be described by the Richardson number for the ocean, which is again defined as the ratio of the static stability N^2 (Eq. 3.8) to the square of the vertical shear of the horizontal current:

$$R_\mathrm{i} = \frac{g}{\overline{\rho}} \frac{\partial \overline{\rho}/\partial z}{(\partial \overline{\mathbf{u}}/\partial z)^2}. \tag{6.31}$$

References

Holton, J. R. (1992), *An Introduction to Dynamic Meteorology*, 3rd ed., 511 pp., Academic Press, London, U.K.

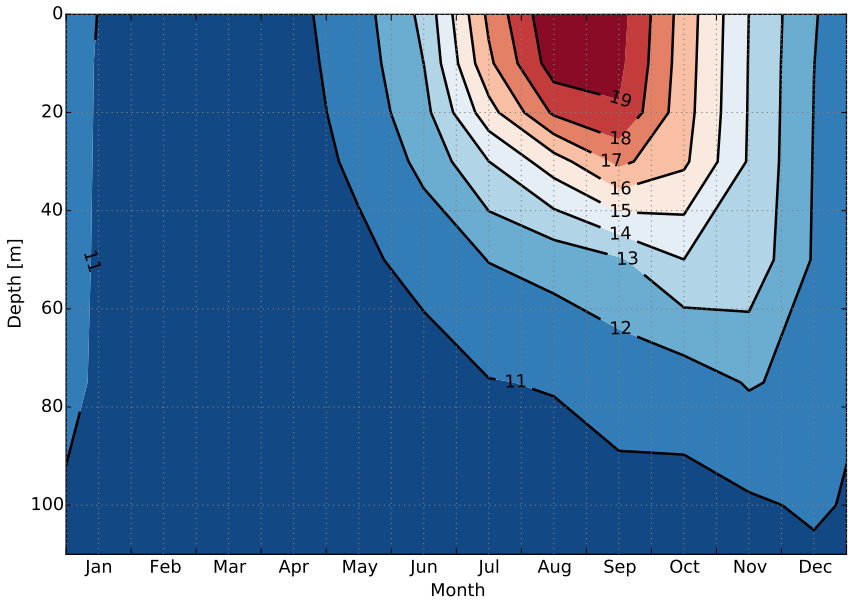

Figure 6.8: The seasonal cycle of temperature in the top 100 m of the Pacific Ocean near 40°N. Data from the World Ocean Atlas 2009. See also Figure 3.4.

Jacobson, M. Z. (2005), *Fundamentals of Atmospheric Modeling*, 2nd ed., 813 pp., Cambridge University Press, Cambridge, U.K.

Sarachik, E. S., and M. A. Cane (2010), *The El Niño–Southern Oscillation Phenomenon*, 369 pp., Cambridge University Press, Cambridge, U.K.

Vallis, G. K. (2006), *Atmospheric and Oceanic Fluid Dynamics*, 745 pp., Cambridge University Press, Cambridge, U.K.